The amplitude phase dynamics and fixed points in tapping-mode atomic force microscopy

Abu Sebastian, Anil Gannepalli, Murti V. Salapaka
Dept. of Electrical & Computer Engineering
Iowa State University
Ames, Iowa 50011

***Abstract*— The first harmonic of the cantilever deflection in the tapping-mode operation of an Atomic Force Microscope (AFM) is analyzed using asymptotic methods for weakly nonlinear oscillators. The resulting amplitude and phase dynamical equations are obtained which characterize the transient behavior of tapping-mode dynamics. The steady state behavior is analyzed by examining the fixed points of the amplitude phase dynamics and a simple stability criterion is obtained. Further with a simple tip-sample interaction model, the experimentally observed discontinuous jumps in the amplitude versus tip-sample separation plots are explained and the regions of the interaction regime probed by the tip are investigated.**

I. Introduction

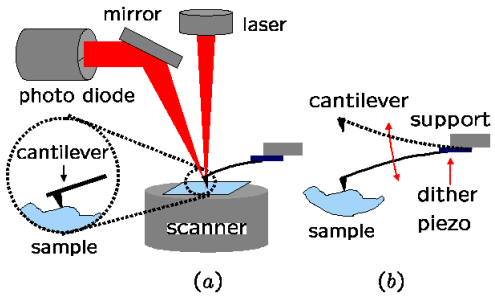

Fig. 1. (a) A typical setup of an AFM. The chief components are the micro-cantilever, a sample positioning system and an optical detection system (b)In tapping-mode AFM, the cantilever is oscillated by a dither piezo attached to the base. Due to tip-sample interaction forces, the oscillations get modulated and these are used to infer the sample characteristics.

The atomic force microscope (AFM) is a powerful tool where a micro-cantilever is utilized to image and manipulate matter at the atomic scale. The schematic of a typical AFM is shown in Figure 1 (a). The primary component of an AFM is a micro-cantilever with a sharp tip. The sample to be interrogated is scanned underneath the cantilever. The cantilever deflects under the influence of the tip-sample interaction forces. This deflection is measured using an optical detection system. Over the years a wide range of modes of operation have emerged. In contact mode or static mode operation, the cantilever deflection is primarily due to the tip-sample interaction and this signal is used to interpret sample properties. In the tapping-mode or dynamic mode operation, the cantilever support is forced sinusoidally using a dither piezo (see Figure 1 (b)) thereby oscillating the cantilever. The changes in the oscillation (in particular the amplitude or phase of the first harmonic) introduced due to the sample are interpreted to obtain the sample properties.

In the tapping-mode operation, the cantilever tip probes a wide range of the nonlinear tip-sample interaction potential. Due to the complexity, numerical simulations are primarily employed in the analysis of tapping-mode AFM dynamics (see [1], [2]). Compared to numerical investigations there are fewer analytical studies of tapping-mode operation.

In [3] and [4] a systems approach to the analysis of tapping-mode AFM dynamics was introduced where the tapping-mode operation was viewed as a feedback interconnection of a linear system (cantilever) with a nonlinear system (tip-sample interaction) which is forced sinusoidally. This analysis provided insights as to why in most operating conditions the cantilever settles down to a near sinusoidal periodic solution. Bounds were obtained for the higher harmonics in the steady state. But this analysis is not suitable to analyze the transient behavior of the tapping-mode dynamics and cannot explain the experimentally observed discontinuous jumps in the amplitude and phase at different values of cantilever-sample separation. Some of the early analytical efforts to explain these distinctly nonlinear phenomena are presented in [5], [6] and [7]. In one of the earliest attempts to characterize the transient behavior of tapping-mode operation, resorting to the averaging theorem, the amplitude phase dynamics were obtained (see [8]). Further the connection between the fixed points of the amplitude phase dynamics and those obtained using harmonic balance equations is presented.

In this article we provide new insights into the transient and nonlinear behavior of tapping-mode AFM. The emphasis of the paper is on tractable analytical methods and interaction models with an eye on potential applications in controller design based on amplitude dynamics and new modes of imaging. There are recent results which give directions to utilize the distinctly nonlinear nature of tapping-mode operation for improved imaging (see [9]). This focus of the paper is different from the interesting efforts to analyze the tapping-mode behavior in an elaborate manner using detailed descriptions for the forcing and interaction models (see [10]). In this paper the oscillating cantilever influenced by the tip-sample interaction force is treated as a weakly nonlinear harmonic oscillator. Methods suggested by Bogoliubov and Mitropolskii (see [11] and [12]) are used to arrive at approximate solutions for the differential equations characterizing the cantilever dynamics.

The amplitude and phase dynamic equations are derived. The multi-valued frequency response curves are obtained and a simple stability criterion is derived to analyze the stability of various fixed points. Insights are obtained on the regions of tip-sample potential probed during tapping-mode operation. This study further demonstrates that a simple lumped parameter model captures the transient as well as steady state behavior.

II. Analysis

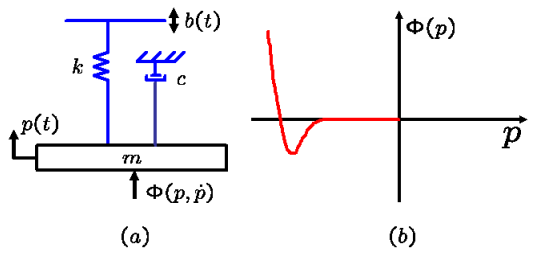

Fig. 2. (a) The first mode approximation of the cantilever dynamics. m is the mass, k is the spring constant, c is the damper, p is the position of the tip of the cantilever, b is the forcing signal and Φ is the nonlinear tip-sample interaction force which is a function of the position and velocity. (b) Typical tip-sample interaction forces consist of long range weak attractive forces and short range strong repulsive forces. In the model introduced, the oscillating cantilever encounters the tip-sample interaction forces during the negative cycle of its oscillation.

A first mode approximation is typically sufficient to analyze the first harmonic of the cantilever oscillation. The first mode approximation model of the cantilever is depicted in Figure 2(a). A typical plot of the nonlinear tip-sample interaction force is shown in Figure 2(b). The dynamical equation of the tip of the cantilever, $p(t)$ is given by,

$$m\ddot{p}+c\dot{p}+kp = kb(t)+\Phi(p,\dot{p}) \tag{1}$$

where Φ is the force on the cantilever due to the sample and b describes the displacement of the base of the cantilever. m is the mass of the cantilever, k, the spring constant and c the damping coefficient. The tip encounters the tip-sample interaction forces towards the end of the negative cycle of the oscillation. Thus during most part of the oscillation cycle the tip does not interact with the sample. This motivates the analysis of tapping-mode dynamics using the asymptotic methods developed for weakly nonlinear systems. In the case of tapping-mode operation the nonlinear forces are significantly higher than the non-contact mode of operation of the AFM, another dynamic mode operation where the tip probes only the attractive regime of the tip sample interaction. However the experimental results presented later validates the assumption that the cantilever sample system can be modeled as a weakly nonlinear oscillator even for the tapping-mode operation.

From Equation 1 it can be observed that in free air the cantilever oscillation is characterized by the parameters k and c since $\Phi = 0$. It is intuitive to assume that due to the tip sample interaction (when Φ is nonzero), the cantilever can still be thought of as a harmonic oscillator with a new effective k denoted by k_e and an effective c denoted by c_e which themselves are functions of the amplitude of oscillation. Furthermore intuitively an attractive tip-sample interaction should result in a lower k_e and a repulsive tip-sample interaction should result in a higher k_e compared to the original k. This process of approximating the original nonlinear dynamical equation by a second order linear differential equation in terms of $k_e(a)$ and $c_e(a)$ is called equivalent linearization. (See [12]).

A. Amplitude phase dynamics

Equation (1) can be recast as,

$$m\ddot{p}+kp = \varepsilon\left(\frac{-c\dot{p}+\Phi(p,\dot{p})}{\varepsilon}\right)+\varepsilon\frac{mg(t)}{\varepsilon} \tag{2}$$

where $g(t)=\frac{kb(t)}{m}$. This can be written as,

$$m\ddot{p}+kp = \varepsilon f(p,\dot{p})+\varepsilon E\cos(\omega t) \tag{3}$$

where

$$f(p,\dot{p}) = \frac{-c\dot{p}+\Phi(p,\dot{p})}{\varepsilon} \tag{4}$$

$$E\cos(\omega t) = \frac{mg(t)}{\varepsilon} \tag{5}$$

Also if $g(t)=\gamma\cos\omega t$ (γ is the forcing amplitude), then $E=\frac{m\gamma}{\varepsilon}$.

Assume that $p(t)$ is sinusoidal with an "amplitude", a and "phase", ϕ denoted by,

$$p(t) = a\cos(\omega t+\phi). \tag{6}$$

where

$$\dot{a} = -\delta_e(a)a-\varepsilon\frac{E\sin\phi}{m(\omega_0+\omega)} \tag{7}$$

$$\dot{\phi} = \omega_e(a)-\omega-\varepsilon\frac{E\cos\phi}{ma(\omega_0+\omega)}. \tag{8}$$

where,

$$\omega_e(a)^2 = \frac{k_e(a)}{m} = \omega_0^2+\frac{2}{a}\overline{\Phi}_c, \tag{9}$$

$\overline{\Phi}_c=\frac{1}{2\pi}\int_0^{2\pi}\frac{\Phi(a\cos\psi,-a\omega\sin\psi)}{m}\cos\psi d\psi$
and

$$\delta_e(a) = \frac{c_e(a)}{2m} = \xi\omega_0+\frac{1}{a\omega}\overline{\Phi}_d, \tag{10}$$

$\overline{\Phi}_d=\frac{1}{2\pi}\int_0^{2\pi}\frac{\Phi(a\cos\psi,-a\omega\sin\psi)}{m}\sin\psi d\psi$

Note that a and ϕ are the amplitude and phase typically referred to in the tapping-mode literature. It could be shown that Equation (6) satisfies Equation (3) with an accuracy of the order ε^2 when the forcing frequency ω is chosen such that $\omega_0^2-\omega^2$ is of order ε (See [11]). The solution is equivalent to that of a linear system with damping coefficient

$c_e(a)$ and spring constant $k_e(a)$ forced by a sinusoidal input at frequency ω. Correspondingly the equivalent resonant frequency is given by $\omega_e(a)$.

Let $\Delta\omega^2 = \frac{2}{a}\overline{\Phi}_c$ and $\Delta c_m = \frac{2}{a\omega}\overline{\Phi}_d$. Δc_m is a measure of the dissipative component of the tip-sample interaction since the energy dissipation in a harmonic oscillator is a function of the damping coefficient. Similarly $\Delta\omega^2$ is a measure of the conservative interaction and could take positive or negative values depending on $\overline{\Phi}_c$. If the sample is conservative, the dissipative component of the tip-sample interaction, $\overline{\Phi}_d = 0$ and $\overline{\Phi}_c$ does not depend on the phase ϕ.

For a fixed tip-sample separation and a fixed forcing frequency, in the transient state the amplitude and phase of the first harmonic of the cantilever oscillation evolve according to (7) and (8) which are nonlinear differential equations unlike in the absence of tip-sample interaction forces.

B. Steady state behavior

In the steady state the amplitude and phase of the first harmonic settles down to one of the fixed points of (7) and (8). The fixed points are given by,

$$-\delta_e(a)a - \varepsilon\frac{E\sin\phi}{m(\omega_0+\omega)} = 0 \quad (11)$$

$$\omega_e(a) - \omega - \varepsilon\frac{E\cos\phi}{ma(\omega_0+\omega)} = 0 \quad (12)$$

We obtain with an accuracy of ε^2,

$$2m\omega\delta_e(a)a = -\varepsilon E\sin\phi \quad (13)$$

$$ma(\omega_e(a)^2 - \omega^2) = \varepsilon E\cos\phi \quad (14)$$

From (13) and (14), we get

$$m^2a^2\{(\omega_e(a)^2-\omega^2)^2 + 4\omega^2\delta_e(a)^2\} = \varepsilon^2E^2 \quad (15)$$

Equation (15) gives the equilibrium points for the amplitude and phase dynamics. For each fixed l (hence a fixed tip-sample interaction potential) and ω, there could be more than one equilibrium point. This is an inherent feature of the nonlinear nature of tapping-mode operation. A purely linear analysis will not be able to explain experimental behavior which is due to this inherent nonlinear behavior. This is in contrast with the contact mode operation where the local nature of the tip-sample interaction forces permits a linear approximation.

Moreover let (a_0,ϕ_0) be an equilibrium point of the dynamical equations (7) and (8). Then the tip sample interaction force signal, $\Phi(t) = \Phi(a_0\cos(\omega t+\phi_0), -a_0\omega\sin(\omega t+\phi_0))$. Let Φ_1 be the first Fourier coefficient of the signal $\frac{\Phi(t)}{m}$. Then it can be shown that $\overline{\Phi}_c = \Phi_{1r}\cos\phi_0 + \Phi_{1i}\sin\phi_0$ and $\overline{\Phi}_d = \Phi_{1r}\sin\phi_0 - \Phi_{1i}\cos\phi_0$ where Φ_{1r} and Φ_{1i} are the real and imaginary parts of Φ_1. This connects the conservative and dissipative components of the interaction force during steady state to the Fourier coefficients of the periodic tip-sample interaction force signal.

C. Conditions for the stability of fixed points

Due to the multiple equilibria, there are chances for discontinuous jumps in amplitude and phase when either the tip-sample separation l is varied for a fixed forcing frequency or when the forcing frequency is varied for a fixed tip sample separation. These discontinuities are frequently observed in experiments and can be explained by analyzing the stability of the fixed points given by equation (15).

Let,

$$R(a,\phi) = -2\omega a\delta_e(a) - \frac{\varepsilon E}{m}\sin\phi \quad (16)$$

$$S(a,\phi) = (\omega_e(a)^2-\omega^2)a - \frac{\varepsilon E}{m}\cos\phi \quad (17)$$

From equation (13) and (14), the fixed points are given by $R(a,\phi)=0$ and $S(a,\phi)=0$. If (a_0,ϕ_0) denote an equilibrium point, then the stability of the equilibrium point is given by the following two conditions,

$$a_0R'_a(a_0,\phi_0) + S'_\phi(a_0,\phi_0) < 0 \quad (18)$$

$$R'_a(a_0,\phi_0)S'_\phi(a_0,\phi_0) - S'_a(a_0,\phi_0)R'_\phi(a_0,\phi_0) > 0 \quad (19)$$

Condition (18) is typically satisfied under usual laws of friction. Hence it suffices to see if (19) is satisfied.

From equation 16, if $R(a,\phi)=0$, then

$$R'_a\frac{da}{d\omega} + R'_\phi\frac{d\phi}{d\omega} = -R'_\omega \quad (20)$$

Similarly from equation 17, if $S(a,\phi)=0$, then

$$S'_a\frac{da}{d\omega} + \phi'_\phi\frac{d\phi}{d\omega} = -S'_\omega \quad (21)$$

From the above two equation,

$$(R'_aS'_\phi - S'_aR'_\phi)\frac{da}{d\omega} = S'_\omega R'_\phi - R'_\omega S'_\phi \quad (22)$$

Also from (16) and (17),

$$R'_\phi = \frac{-\varepsilon E}{m}\cos\phi$$
$$R'_\omega = -2a\delta_e(a)$$
$$S'_\phi = \frac{\varepsilon E}{m}\sin\phi$$
$$S'_\omega = -2\omega a$$

Hence the right hand side of equation (22) is given by

$$S'_\omega R'_\phi - R'_\omega S'_\phi = (-2\omega a)\frac{-\varepsilon E}{m}\cos\phi - (-2a\delta_e(a))\frac{\varepsilon E}{m}\sin\phi$$
$$= 2a^2\omega\{(\omega_e(a)^2-\omega^2) - 2\delta_e(a)^2\}$$

From the above discussion we get,

$$(R'_aS'_\phi - S'_aR'_\phi)\frac{da}{d\omega} = 2a^2\omega\{\omega_e(a)^2 - (\omega^2+2\delta_e(a)^2)\} \quad (23)$$

Note that $R'_aS'_\phi - S'_aR'_\phi$ when evaluated at a fixed point (a_0,ϕ_0) is the quantity which should be always positive under the second stability condition given by equation 19. So (23) can be interpreted as the following. If one has a plot of the fixed point amplitudes versus the frequency of forcing, then a particular fixed point amplitude a_0 is stable

if $\frac{da}{d\omega}|_{a=a_0}$ is greater than zero when $\omega_e(a)^2 > \omega^2 + 2\delta_e(a)^2$ and $\frac{da}{d\omega}|_{a=a_0}$ is less than zero when $\omega_e(a)^2 < \omega^2 + 2\delta_e(a)^2$. If the damping is very small, then a fixed point amplitude is stable if the slope at the point is positive for forcing frequencies below the equivalent resonant frequency and the slope is negative for forcing frequencies above the resonant frequency.

III. Experimental Results and Discussion

Experiments were performed on a *Digital Instruments* Multimode AFM. A silicon cantilever with natural frequency 335.4 *kHz* was chosen. The deflection signal was sampled at 5 *MHz*. The cantilever parameters were identified from the thermal noise response of the cantilever.

The cantilever was oscillated at the frequency $f_0 = 335.4$ *kHz* to an amplitude of 24.25 *nm*. The sample (Highly Oriented Pyrolitic Graphite (HOPG)) was moved towards the freely oscillating cantilever and then away. The cantilever oscillation during this process as a function of the time is depicted in Figure 3. If the position of the tip $p(t)$ is assumed to be $a\cos(\omega t + \phi)$ where $\omega = \omega_0 = 2\pi f_0$, then the resulting amplitude, a is plotted against the tip-sample separation l (see Figure 4). The approach and retraction of the sample is performed sufficiently slow so that the amplitude and phase evolving according to (7) and (8) settle to an equilibrium amplitude and phase for a particular tip-sample separation. Note that there is some ambiguity about the absolute tip-sample separation which will be addressed when a model is introduced for the tip-sample interaction.

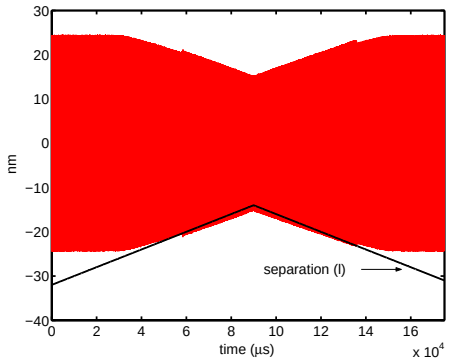

Fig. 3. The cantilever deflection signal is plotted as a function of time when the sample is moved towards and then away from the oscillating tip. The tip-sample separation is also plotted as a function of the time.

When the cantilever is freely oscillating, the amplitude is 24.25 *nm*. As the sample is moved towards the oscillating tip, at a separation of 20.33 *nm*, the amplitude jumps to a higher value for an arbitrarily small decrease in the tip-sample separation. Similarly as the sample is moved away from the tip, at a separation of 23.2 *nm*, for an arbitrarily small increase in tip sample separation the amplitude drops down to a lower value. These discontinuous jumps can be explained using the multi-valued frequency response curve as discussed in the previous section.

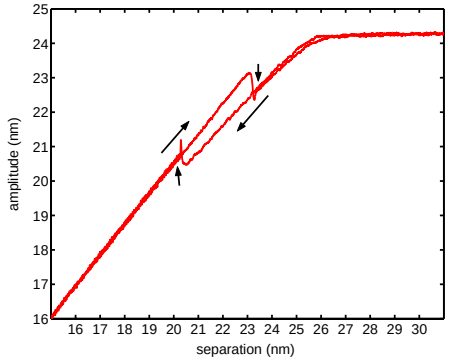

Fig. 4. The amplitude is plotted as a function of the tip-sample separation. When the sample is approaching the oscillating tip, the cantilever jumps to a higher amplitude at a tip-sample separation of 20.33 *nm*. While retracting, the amplitude drops to a lower amplitude at a tip-sample separation of 23.2 *nm*.

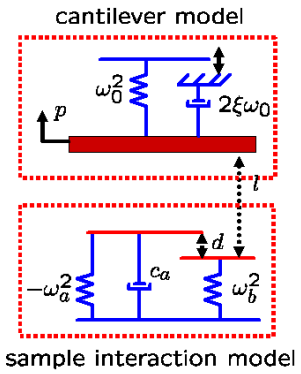

Fig. 5. The tip-sample interaction forces are characterized by long range attractive forces and short range repulsive forces. A negative spring is used to model the attractive forces and a positive spring is used to model the repulsive forces. The tip-sample separation l is defined to be distance between the tip and the beginning of the repulsive spring. The length of the attractive region, d is the separation between the attractive and repulsive springs. The damping in the sample is captured by a damper.

In order to analyze this behavior a simple model is developed for the tip-sample interaction force. This is first introduced in [3]. Figure 5 depicts the models for the cantilever and the tip-sample interaction force. The tip-sample interaction force has long range attractive and short range repulsive components. The model parameters are normalized for unit mass. The long range attractive component is modeled by a negative spring denoted by $-\omega_a^2$. The repulsive component is modeled by a positive spring denoted by ω_b^2. The dissipation in the sample is captured by a damper denoted by c_a. l is a good measure of the tip-sample interaction forces and is the distance between the tip and the beginning of the repulsive regime. d is the length of the attractive regime. Using the identification schemes described in [3], ω_a, ω_b, c_a and d were estimated for the experimental data. $\omega_a = 0.765\ \mu s^{-1}$, $\omega_b = 3\ \mu s^{-1}$, $c_a = 0.017\ \mu s^{-1}$ and $d = 2.55$ *nm*. Using these parameters simulation were performed and the resulting amplitude versus separation data is compared with the experimental

results in Figure 6.

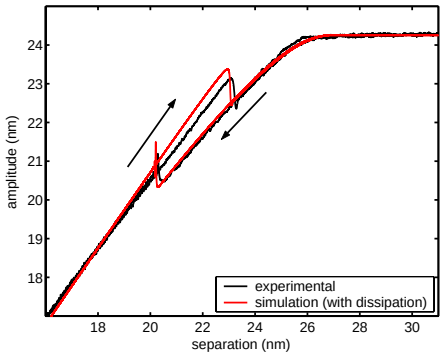

Fig. 6. The amplitude versus tip-sample separation curve is obtained using the interaction model and is compared with that obtained from experiments. There is remarkable agreement between the two. The discontinuities are observed in both plots.

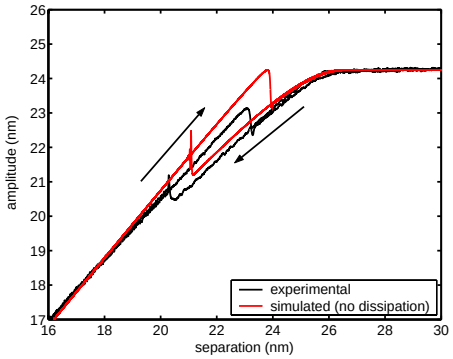

Fig. 7. To simplify the analysis, the sample is assumed to be conservative or non-dissipative. The simulation results still agree with the experimental results qualitatively and show the discontinuities.

Note that there is remarkable similarity between the experimental data and those obtained through simulations. For simplifying the future discussion, the damping term c_a is assumed to be zero in the model. This brings about a minor discrepancy with the experimental data as shown in Figure 7. This assumption means there is no additional damping due to the introduction of sample. There is a loss of generality as seen in the mismatch between the experimental and simulation data depicted in Figure 7. But this simplifies the analysis at the same time retaining the essential features.

The multi-valued frequency response and the stability of the resulting multiple equilibria when forced at a particular forcing frequency (the resonant frequency in this case) can explain the discontinuities present in the amplitude versus separation plot. The multi-valued frequency response curves at different tip-sample separations are depicted in Figure 8 for the model developed earlier. These curves are obtained by solving for Equation (15). When the oscillating cantilever is away from the sample surface, it can be modeled as a linear system with a single valued frequency response curve. As shown in Figure 8 ($l = 24.5$), in the attractive

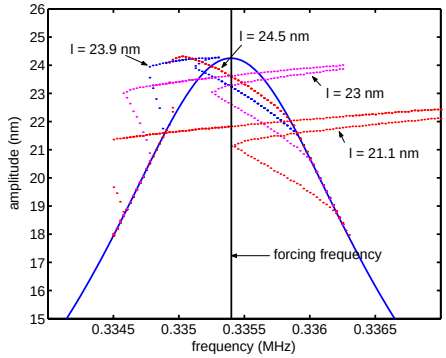

Fig. 8. For different tip-sample separations, the multi-valued frequency response curves are obtained by solving Equation 15.

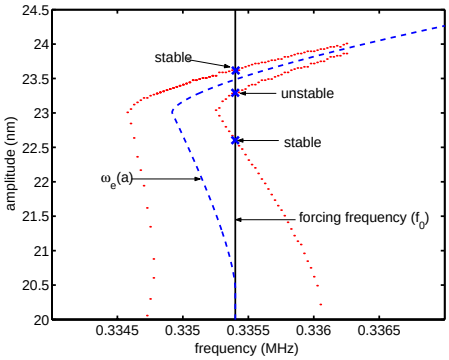

Fig. 9. For a tip-sample separation of $l = 23$ *nm*, the multi-valued frequency response curve is shown. For a forcing frequency of f_0, there are three possible fixed point amplitudes. From the stability criteria two of the three are stable.

regime the frequency response curve starts becoming multi-valued and will have a slant towards a frequencies lower than the free resonant frequency. But since the cantilever is being forced at the resonant frequency there is still only one equilibrium point. But this scenario changes once the repulsive forces start influencing the oscillating tip. For example for a separation of 23 *nm*, at the forcing frequency there are three equilibrium points as depicted in Figure 8 and separately in Figure 9. From the stability analysis of the previous section two of the three equilibrium amplitudes are found to be stable. The equivalent resonant frequency $\omega_e(a)$ is evaluated as a function of the amplitude for the tip-sample interaction model and is shown in Figure 9. If the forcing frequency ω is greater than $\omega_e(a)$, then the slope $\frac{da}{d\omega}$ has to be negative and if the forcing frequency ω is less than $\omega_e(a)$, then the slope $\frac{da}{d\omega}$ has to be positive for an equilibrium amplitude to be stable.

The discontinuities in the amplitude versus separation plot can be explained in terms of the multi-valued frequency response plots, the resulting multiple equilibrium amplitudes and their stability. As the sample approaches the oscillating tip, the amplitude remains on the lower branch till the separation $l = 21.1nm$ (see Figure 8. At this

point, the amplitude is forced to jump to a higher value, 21.5 *nm* from the lower value of 21.1 *nm* as there is only one equilibrium amplitude for tip-sample separation values below $l = 21.1nm$. While moving away from the oscillating tip, the amplitude will remain on the higher branch till when the separation $l = 23.9$ *nm* when the amplitude is forced to drop to 23.1 *nm* from 24.2 *nm* since for the tip-sample separations above $l = 23.9$ *nm*, there is only one equilibrium amplitude when forced at ω_0. Note that the amplitude never takes the value between the high and low values since those equilibrium amplitudes are unstable.

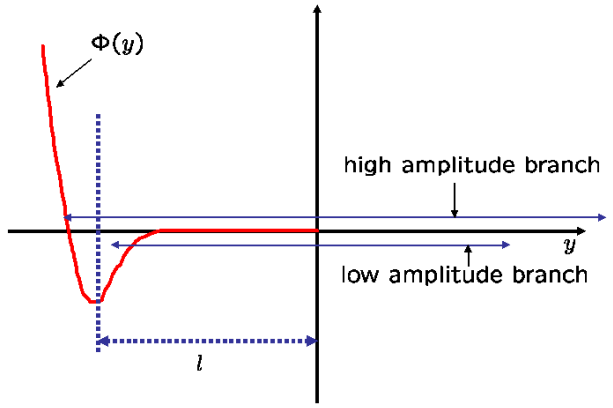

Fig. 10. In tapping mode operation, the oscillating tip is found to either traverse only the attractive regime (low amplitude branch) with an amplitude less than the tip-sample separation or traverse the attractive and repulsive regimes (high amplitude branch). When the tip-sample separation equals the oscillation amplitude the tip jumps in a discontinuous fashion from the low amplitude branch to the high amplitude branch.

It is useful to analyze the regions of the tip-sample forces the oscillating cantilever probes at different tip-sample separations. From the force curves (both experimental and theoretical) the oscillating tip is found to either traverse only the attractive regime (low amplitude branch) with an amplitude less than the tip-sample separation (as defined by the above model) or traverse the attractive and repulsive regimes (high amplitude branch). When the tip-sample separation equals the oscillation amplitude the tip jumps in a discontinuous fashion from the low amplitude branch to the high amplitude branch (see figure 10. For the same tip-sample separation, the cantilever could be in the low amplitude (attractive region) branch or in the high amplitude (repulsive region) branch depending on whether that particular tip-sample separation was achieved by bringing the sample closer to the tip or by moving the sample away from the tip.

IV. Conclusions

In the tapping-mode operation of the AFM, the cantilever tip traverses a wide regime of the nonlinear tip-sample interaction forces and hence a linear analysis is not sufficient to delineate the salient features. However since the oscillating tip encounters the nonlinear sample interaction forces only for a small fraction of the total oscillation time, averaging methods can be used to analyze the tapping-mode dynamics. Correspondingly an approximate solution is obtained for the cantilever oscillation where the amplitude and phase of the first harmonic evolves according to a nonlinear differential equation. The transient behavior of tapping-mode operation is captured by these equations. The steady state values for amplitude and phase are given by the fixed points of these amplitude phase dynamical equations. With a simple tip-sample interaction model and the stability of these fixed points some of the experimentally observed behavior of tapping-mode operation is explained. It is surprising that a piecewise linear interaction and an analysis which assumes the tip-sample system to be weakly nonlinear (which appears to be simplistic for tapping-mode operation where the interaction forces are quite significant) explains the experimental behavior in a remarkable manner.

V. Acknowledgements

This research is supported by National Science Foundation Grant ECS-0330224 to Prof. Murti V. Salapaka.

References

[1] B. Anczykowski, D. Kruger, K. L. Babcock, and H. Fuchs, Basic properties of dynamic force spectroscopy with scanning force microscope in experiment and simulation, *Ultramicroscopy*, vol. 66, 1996, pp. 251.

[2] M. Marth, D. Maier, J. Honerkamp, R. Brandsch, and G. Bar, A unifying view on some experimental effects in tapping-mode atomic force microscopy, *Journal of Applied Physics*, vol. 85 (10), 1999, pp. 7030.

[3] A. Sebastian, M. V. Salapaka, D. J. Chen, and J. P. Cleveland, Harmonic and power balance tools for tapping-mode atomic force microscope, *Journal of Applied Physics*, vol. 89 (11), 2001, pp. 6473.

[4] A. Sebastian and M. V. Salapaka, "Analysis of periodic solutions in tapping-mode afm: An IQC approach", *in International sysmposium on Mathematical Theory of Networks and Systems*, South Bend, IN, August 2002.

[5] L. Wang, Analytical descriptions of the tapping-mode atomic force microscopy response, *Applied Physics Letters*, vol. 73 (25), 1998, pp. 3781.

[6] M. Gauthier, N. Sasaki, and M. Tsukada, Dynamics of the cantilever in noncontact dynamic force microscopy: The steady-state approximation and beyond, *Physical Review B*, vol. 64, 2001, pp. 85409.

[7] A. San Paulo and R. Garcia, Tip-surface forces, amplitude and energy dissipation in amplitude-modulation (tapping mode) force microscopy, *Physical Review B*, vol. 64, 2002, pp. 41406.

[8] A. Sebastian, M. V. Salapaka, D. J. Chen, and J. P. Cleveland, "Harmonic analysis based modeling of tapping-mode AFM", *in Proceedings of the American Control Conference*, San Diego, California, June 1999.

[9] R. W. Stark, G. Schitter, and A. Stemmer, Tuning the interaction forces in tapping mode atomic force microscopy, *Physical Review B*, to be published.

[10] S. I. Lee, S. W. Howell, A. Raman, and R. Reifenberger, Nonlinear dynamics of microcantilevers in tapping mode atomic force microscopy: A comparison between theory and experiment, *Physical Review B*, vol. 66, 2002, pp. 115409.

[11] N. N. Bogoliubov and Y. A. Mitropolskii, *Asymptotic methods in the theory of non-linear oscillations*, Hindustan publishing corporation, New Delhi, India; 1961.

[12] Y. A. Mitropolskii and N. Van Dao, *Applied asymptotic methods in non-linear oscillations*, Kluwer academic publishers, The Netherlands; 1997.